Landscape Ecol (2016) 31:745–760
DOI 10.1007/s10980-015-0284-3

RESEARCH ARTICLE

Micro-scale urban surface temperatures are related to land-cover features and residential heat related health impacts in Phoenix, AZ USA

G. Darrel Jenerette · Sharon L. Harlan · Alexander Buyantuev · William L. Stefanov · Juan Declet-Barreto · Benjamin L. Ruddell · Soe Win Myint · Shai Kaplan · Xiaoxiao Li

Received: 10 September 2014 / Accepted: 28 September 2015 / Published online: 19 October 2015

Abstract
Context With rapidly expanding urban regions, the effects of land cover changes on urban surface temperatures and the consequences of these changes for human health are becoming progressively larger problems.
Objectives We investigated residential parcel and neighborhood scale variations in urban land surface temperature, land cover, and residents' perceptions of landscapes and heat illnesses in the subtropical desert city of Phoenix, AZ USA.
Methods We conducted an airborne imaging campaign that acquired high resolution urban land surface temperature data (7 m/pixel) during the day and night. We performed a geographic overlay of these data with high resolution land cover maps, parcel boundaries, neighborhood boundaries, and a household survey.
Results Land cover composition, including percentages of vegetated, building, and road areas, and values for NDVI, and albedo, was correlated with residential parcel surface temperatures and the effects differed between day and night. Vegetation was more effective at cooling hotter neighborhoods. We found

G. D. Jenerette (✉)
Department of Botany and Plant Sciences, University of California Riverside, Riverside, CA, USA
e-mail: darrel.jenerette@ucr.edu

S. L. Harlan · J. Declet-Barreto
School of Human Evolution and Social Change, Arizona State University, Tempe, AZ, USA

A. Buyantuev
Department of Geography and Planning, University at Albany, State University of New York, Albany, NY, USA

W. L. Stefanov
Astromaterials Research and Exploration Science Division, Exploration Integration and Science Directorate, NASA Lyndon B. Johnson Space Center, Houston, TX, USA

J. Declet-Barreto
Natural Resources Defense Council, Washington, DC, USA

B. L. Ruddell
Fulton Schools of Engineering, Arizona State University, Tempe, AZ, USA

S. W. Myint
School of Geographical Sciences and Urban Planning, Arizona State University, Tempe, AZ, USA

S. Kaplan
The Jacob Blaustein Institutes for Desert Research, Ben-Gurion University of the Negev, Beersheba, Israel

X. Li
Julie Ann Wrigley Global Institute of Sustainability, Arizona State University, Tempe, AZ, USA

consistencies between heat risk factors in neighborhood environments and residents' perceptions of these factors. Symptoms of heat-related illness were correlated with parcel scale surface temperature patterns during the daytime but no corresponding relationship was observed with nighttime surface temperatures.
Conclusions Residents' experiences of heat vulnerability were related to the daytime land surface thermal environment, which is influenced by micro-scale variation in land cover composition. These results provide a first look at parcel-scale causes and consequences of urban surface temperature variation and provide a critically needed perspective on heat vulnerability assessment studies conducted at much coarser scales.

Keywords Urban heat island · Parcel · MASTER · Land surface temperature · Social surveys · Vulnerability

Introduction

Urbanization is associated with increasing air temperatures in cities (Oke 1973), and it also leads to land surface warming and increasing land surface temperature (LST) heterogeneity (Voogt and Oke 2003; Jenerette et al. 2007; Cao et al. 2010; Imhoff et al. 2010; Peng et al. 2012; Zhou et al. 2014). Studies of urban LST have primarily evaluated midday spatial variation at neighborhood or coarser scales, such as the city, zip code, and census tract boundaries. However, extensive scale-dependent variation in LST is expected throughout any given day due to different speeds of warming within the complex spatial structure of urban environments (Li et al. 2011; Weng et al. 2011). Furthermore, the human consequences of urban LST warming are not well characterized at very fine spatial resolutions, such as individual residential parcels, although several studies have found LST variation affects spatial variability in the risk of heat-related mortality at neighborhood scales (Johnson et al. 2009; Buscail et al. 2012; Hondula et al. 2012; Johnson et al. 2012; Harlan et al. 2013).

LST spatial variation is influenced by material properties such as heat capacity, thermal conductivity, and thermal inertia (Elachi 1987), and several studies have proposed that local land cover composition is a primary determinant of LST patterns (Li et al. 2011; Connors et al. 2013; Zhou et al. 2014). Increasing vegetated land cover has been repeatedly shown to lower LST through radiation interception and shading and increases in latent heat fluxes associated with transpiration (Jenerette et al. 2007; Kalma et al. 2008; Kustas and Anderson 2009; Jenerette et al. 2011; Xiang et al. 2014; Zhou et al. 2014). In contrast, built surfaces, including buildings and roads, are generally warmer than natural surfaces (Buyantuyev and Wu 2010; Zhou et al. 2014). Several studies have shown that measurement scale affects the amount of observed variability in land cover—LST relationships (Liang and Weng 2008; Weng et al. 2011; Song et al. 2014), but relationships between urban land cover and LST have almost exclusively been evaluated using satellite-based thermal sensors on Landsat ETM+ (60 m pixels) or ASTER (90 m pixels) instruments (e.g. Li et al. 2011; Myint et al. 2013; Song et al. 2014). At these resolutions, extensive mixing of land covers may obscure stronger or different relationships at finer resolutions where more urban land cover variability occurs (Zhou et al. 2011). An evaluation of urban LST variation at micro scales, such as <10 m, has been noted as an important research goal for improved understanding of the biophysical causes urban heat vulnerability (Small 2003; Deng and Wu 2013; Zhan et al. 2013; Song et al. 2014).

In addition to improved spatial resolution, extending LST measurements to both daytime and nighttime allows for analysis of the differences in causes and consequences of spatial patterns of daily maximum and minimum urban LST (Buyantuyev and Wu 2010; Myint et al. 2013). Because vegetation and high albedo surfaces are cooler during the day and built surfaces are warmer, these trends may continue at night due to differences in stored heat (Buyantuyev and Wu 2010; Myint et al. 2013). Alternatively, trees may trap infrared radiation at night and lead to increased surface warming. Although the upward facing built materials are warmer during the day, they may more effectively radiate heat at night, leading to lower nighttime LST while still radiating heat horizontally. Albedo, as a property associated with an illuminated surface, may be unrelated to nighttime LST. Improved understanding of the biophysical drivers of urban LST will require reconciling the differences in day and night LST variation.

Characterizing the biophysical basis of LST spatial and temporal variations and connecting LST with residents' lived experiences should help us to better understand the determinants of variability in heat vulnerability and implement better climate adaptation strategies for cities. In the large literature that examines air temperature and heat-related mortality, there is considerable discussion and debate about the relative importance of daily and lagged minimum, mean, and maximum temperature effects on health outcome (Kalkstein 1991; Basu and Samet 2002; Hondula and Barnett 2014; Petitti et al. 2015). Studies in different places and weather conditions have reached different conclusions. The important question about the effects of minimum and maximum temperatures has rarely been evaluated using urban LST because there have been many fewer studies that consider LST and most of them exclusively used either daytime (e.g. Harlan et al. 2013) or nighttime data (Uejio et al. 2011). One exception was Laaidi et al. (2012), who examined minimum, mean, and maximum surface temperatures, and found that minimum temperature was associated with heat deaths among the elderly during a heat wave in Paris. As these authors pointed out, variability in surface temperatures measured over the extent of the city more closely approximates the actual living conditions of urban residents than air temperature measured at weather stations that are not in close proximity to people (Laaidi et al. 2012).

In this study, we present new results from high resolution (7 m) airborne thermal imagery acquired over the Phoenix, AZ USA metropolitan region. We link this high resolution thermal data with social survey data on perceptions of landscapes and heat illnesses that were collected during the same year. We use the geographic intersection of these data in conjunction with a sub-meter land cover classification and residential parcel boundaries to answer two questions: (1) How does landscape composition influence LST variability during the day and night at parcel and neighborhood scales? (2) Do parcel and neighborhood surface characteristics correspond to residents' perceptions of their local landscapes and self-reported symptoms of heat-related illnesses? Answering these questions will improve understanding of how land-cover patterns influence LST in residential environments and the potential consequences of LST for residents. These are essential pieces of the puzzle for designing neighborhoods that reduce human vulnerability to increasing urban temperatures.

Methods

Site description

The Phoenix, AZ USA metropolitan region (population 4.3 million) is a well-studied model system that has been useful for learning about many aspects of urban ecology and climate (Grimm and Redman 2004; Chow et al. 2012). This metropolis has a hot, subtropical desert climate (Koppen classification BWh) and features substantial variation in vegetation and built surfaces associated with residential dwellings. Phoenix is an extreme endpoint of the urban heat spectrum within the United States (Stone 2012). The region has a pronounced nighttime urban heat island (UHI) (Chow et al. 2012), measured in air temperature and LST, and is home to one of the fastest growing UHIs within the United States (Stone 2012). Overall, and consistent with cities throughout the southwestern United States, the city has more vegetation than the outlying desert and higher-income neighborhoods (census tracts) have more vegetation than lower-income neighborhoods (Jenerette et al. 2013). Vegetation, in turn, is correlated with LST and higher-income neighborhoods are cooler (Jenerette et al. 2007; Buyantuyev and Wu 2010; Jenerette et al. 2011).

Microscale LST: MASTER flight and data processing

We conducted an airborne LST data collection campaign over the Phoenix metropolitan area during a 5-day period in 2011: July 12–13 (daytime flights collected from 10 am to 1 pm local time; −7 from UTC) and July 15–16 (nighttime flights collected from 12:30–3 am local time). These times were selected to be representative of mid-day and mid-night periods outside the main transitions associated with sunrise or sunset. For this campaign the MODIS/ASTER Simulator, or MASTER, instrument was mounted on a Beechcraft B-200 aircraft and flown to obtain high spatial resolution data. The MASTER sensor acquires data over the visible through mid-infrared wavelengths (0.46–12.817 μm) in 50 spectral bands (Hook et al. 2001), which were used to derive LST, normalized difference vegetation index (NDVI), and albedo at approximately 7 m/pixel. These imagery data measure a combination of the top of urban canopy and ground data, which may be distinct from temperature patterns only at the ground (Goldreich 2006). Although the original intent was to collect a true diurnal dataset, this was not possible due to the large area of data collection and pilot flight rules that constrain daily flying time and mandate stand-down periods for flight safety. Fortuitously, a stable weather pattern prevailed during the week of July 12 that enabled collection of an approximate diurnal dataset. During this period, mean daily maximum air temperature was 40.1 °C and differed less than 1.6 °C between sampling days.

We performed atmospheric correction to obtain apparent surface reflectance, temperature, and emissivity, which allows for comparison of the flight line data collected on four different days. The ENVI/IDL image processing environment was used to perform all processing of the MASTER data. Atmospheric correction of the mid-infrared wavelength data was accomplished using an in-scene atmospheric compensation technique (Johnson and Young 1998). We used an emissivity normalization approach (Kealy and Hook 1993) to obtain LST from the MASTER data—an emissivity value of 0.98 was used to calculate the temperature in each band of the MASTER thermal IR data for each pixel, and then the highest temperature obtained was used to create the LST layer. That temperature was then used to invert the Planck function to calculate emissivity in each of the bands. Atmospheric correction of the visible through shortwave infrared wavelength data was accomplished using the quick atmospheric correction (QUAC) algorithm (Bernstein et al. 2005) within ENVI/IDL. Reasonableness of both LST and apparent reflectance results were assessed qualitatively by random examination of returned pixel values (surface temperature) and image spectra (vegetation and soil pixel spectra were compared to laboratory spectra of similar materials).

In addition to LST we also processed MASTER data to obtain the NDVI, a measure of vegetation (Tucker 1979), and an estimate of surface albedo. NDVI was calculated as follows:

$$\mathrm{NDVI} = (\mathrm{Band9} - \mathrm{Band5})/(\mathrm{Band9} + \mathrm{Band5})$$

where Band9 and Band5 correspond to MASTER spectral channels 9 (0.87 µm) and 5 (0.66 µm). Albedo, the ratio of upwelling to downwelling radiative flux at the surface, was estimated by converting narrowband to broadband albedo using an empirical formula previously developed for the MODIS sensor (Liang 2001). Specifically, we derived the total visible broadband albedo (α_{vis}) as follows

$$\alpha_{vis} = 0.331\alpha_5 + 0.424\alpha_1 + 0.246\alpha_3$$

where α_1, α_3, and α_5 are reflectances in MASTER spectral channels 1 (0.46 µm), 3 (0.54 µm), and 5 (0.66 µm), respectively.

Phoenix Area Social Survey

The 2011 Phoenix Area Social Survey (PASS) was the second wave of a household survey conducted every 5 years in the metropolitan area to study human-environment interactions in an urban setting. It is part of the long-term monitoring conducted by the Central Arizona—Phoenix Long-Term Ecological Research (CAP LTER) project (http://caplter.asu.edu/research/long-term-monitoring/). A two-stage sampling design was used for PASS. First, the sample of PASS neighborhoods was drawn mostly from long-term ecological monitoring sites that are part of the CAP LTER project (Grimm and Redman 2004). U.S. Census Bureau block groups (i.e., relatively homogeneous populations living within an area of approximately 0.65 km^2) were used to define boundaries of PASS neighborhoods. We selected a sample of 45 PASS neighborhoods (39 from long-term monitoring sites and six other CAP LTER research sites) stratified by location (urban, suburban, fringe) and median household income. Percent retired and percent minority residents were also considered in the selection to ensure that different types of residential situations were represented (Table 1).

Second, the sampling frame for households within each neighborhood was a list of eligible residential addresses created from maps and the tax assessor's parcel numbers (APN), which included single family and multi-family houses, apartment buildings, and mobile home parks. A random sample of 40 households was selected within each neighborhood. Respondents were offered a small financial incentive for participation and they could complete the survey online, by telephone, or in person with an interviewer. All materials were available in English and Spanish and repeated follow-up efforts with non-respondents were on-going through the study period. A total of 806

Table 1 Stratification of the 2011 Phoenix Area Social Survey neighborhoods and survey respondents

Neighborhood classification	Neighborhoods (n)	Respondents (n)
Low income, urban core	6	97
Low income, suburban	6	110
Low income, fringe	2	34
Subtotal low income	14	241
Middle income, urban core	6	105
Middle income, suburban	6	111
Middle income, fringe	7	136
Subtotal middle income	19	352
High income, urban core	1	20
High income, suburban	5	94
High income, fringe	6	99
Subtotal high income	12	213
Grand total	45	806

Median annual household income for each neighborhood was obtained from 2000 U.S. Census block group data and classified as follows: low income (<\$35,000); middle income (\$35,000–\$70,000); high income (>\$70,000). Urban core neighborhoods were within 8 km of downtown Phoenix or within 2.4 km of the 7 other large-city downtowns. Fringe areas had a moderate amount of undeveloped land within 1.6 km of the neighborhood in 2005. All other neighborhoods were classified as suburban. At least 30 % of residents in five neighborhoods were 65 years or older in 2010 (retirement communities) and at least 50 % of residents in ten neighborhoods were non-Hispanic white (Hispanic, African American, Native American, or Asian/Pacific Islander) in 2010

respondents in 45 neighborhoods, ages 18 or older (one per household), completed the survey for a minimum response rate of 43.4 % using the standard definitions of the American Association for Public Opinion Research (2008). All surveys were completed between May 26 and December 31, 2011.

The survey asked respondents' opinions about quality of life and condition of the natural environment in their neighborhoods and in the region. Questions about land use and climate were two areas of emphasis. We selected three questions from PASS as indicators of residents' perceptions of environmental conditions in their neighborhoods and one question on self-reported heat illnesses (Table 2). The question about experiencing heat-related symptoms was asked in the survey context of 10 other questions about heat and the symptoms we included in the question (Table 2) were excerpted from the medical conditions directly attributable to excessive heat exposure

Table 2 Responses of participants to questions in the 2011 Phoenix Area Social Survey (n = 806)

Survey question	Response %	Response n
During the summer of 2010, do you think your neighborhood was (_) than most other neighborhoods in the Valley?		
A lot cooler	0.9	7
A little cooler	14	117
About the same temperature	22	174
A little hotter	9.4	76
A lot hotter	45	366
Are you (_) with trees that provide shade in your neighborhood?		
Very satisfied	27	215
Somewhat satisfied	36	292
Somewhat dissatisfied	22	178
Very dissatisfied	13	106
Please indicate whether having too many paved surfaces such as roads or parking lots is a (_) in your neighborhood		
Big problem	5.8	47
Little problem	18	142
Not a problem at all	74	594
During last summer, did anyone in your household have symptoms related to heat or high temperatures such as leg cramps, dry mouth, dizziness, fatigue, fainting, rapid heartbeat or hallucinations?		
Yes	30	245
No	60	486
Do any of the following prevent you from using your air-conditioning *when the weather is hot*? Please select all that apply		
Cost of electricity	36	291
Unit doesn't work	5.3	43
Cost of repairs	4.1	33
Noise	1.0	8
Do not have an air conditioner	3.6	29
Other	1.9	15
Summary: had at least one impediment	45.3	365

Missing and "don't know" answers were omitted from calculations on an item-by-item basis and 100 % was based on number of valid answers for each question, or in the case of the question on impediments to using air conditioning, valid answers for each item. (For the question on use of air conditioning, respondents could select multiple answers). Responses to the question on neighborhood temperature were coded so that higher scores indicate hotter neighborhood relative to others. Responses to the question on satisfaction with trees were coded so that higher scores indicate higher satisfaction. Responses to the question on too much pavement were coded so that higher scores indicate a smaller problem (higher satisfaction). Subsamples of respondents in neighborhoods that correspond to useable imagery from the daytime and nighttime MASTER land cover dataset (n = 640 and 695, respectively) were used in the analyses (see "Geoprocessing: MASTER georectification and data overlays" section) published by the United States Environmental Protection Agency (2006, p. 11). Self-rated health questions are widely used in the health sciences and other fields because, over decades of research, they have been found to be strong correlates of clinical conditions (Lee 2015) and have been used in assessments of heat vulnerability (Belanger et al. 2015).

In evaluating the effect of LST on respondents' reported experiences with heat illness, we used a question about economic impediments to home air conditioning. Regulating indoor temperatures with air conditioning is an important method of coping with extreme outdoor temperatures in Phoenix and inability to access this coping mechanism could increase the likelihood of heat illness. We tested for a potentially confounding effect of ambient outdoor temperature on respondents' answers to the heat illness question by evaluating the influence of maximum air temperature (obtained from Sky Harbor Airport) on the survey response date. The Arizona State University Institutional Review Board approved the use of PASS data for this study.

Geoprocessing: MASTER georectification and data overlays

For this study, MASTER data were extracted for 41 (out of the total 45) PASS neighborhoods within the flight boundary. The atmospherically corrected MASTER data were processed to at-sensor radiance but did not include geolocation data. We georeferenced each neighborhood to align with the corresponding National Agriculture Imagery Program (NAIP) data. This process included visually locating and matching feature points in the MASTER image and the base NAIP image. These feature points were used to create a polynomial geometric transformation model that aligned the MASTER image to the same coordinate system of the base image. In addition we incorporated a nearest neighbor resampling so that corresponding pixels represent the same objects. For each neighborhood, a different number of matching points was used depending on its size and level of distortion in the MASTER data. All neighborhoods were georeferenced to a target registration error of no more than 0.5 pixels. In cases where severe distortions of the original MASTER data did not allow registration to this level of accuracy, registration to the lowest possible error was performed. In four neighborhoods the daytime thermal images were too distorted for acceptable georeferencing; these highly distorted images were not included in further analyses. Registration of the higher resolution visible reflectance data precluded the use of two more neighborhoods for NDVI or albedo data. The final processed MASTER dataset included high spatial resolution LST, NDVI, albedo, and direct estimates of emissivity that were atmospherically corrected, and georeferencing (Fig. 1).

We linked the MASTER and PASS data with a high resolution (1 m) land cover classification for the Phoenix metropolitan region, which had a classification accuracy of 92 % and a kappa statistic of 0.91 (Li et al. 2014). This classification was conducted using NAIP aerial photography and following an object-oriented expert rule algorithm (Baatz et al. 2008), which is becoming increasingly common for urban regions (Myint et al. 2011; Grove et al. 2014). Preliminary analyses showed that 2.8 % of parcels had no observed built land cover. The presence of trees above the built surface may have obscured buildings and there may also have been errors in the NAIP data or land cover classification. We overlaid the land cover classification and MASTER data with parcel boundaries obtained from the Maricopa County Tax Assessors office and extracted all residential plots (Fig. 2). A complete geographic overlay of land cover, LST, and parcel boundaries for 37 PASS neighborhoods during the day (n parcels = 21,589 and n survey respondents = 640) and 41 neighborhoods at night (n parcels = 25,011 and n survey respondents = 695) was available for our analyses.

Image acquisition occurred over approximately a 3-h flight period and therefore we evaluated the potential for LST to increase during daytime sampling and decrease during nighttime sampling. We compared means across all parcels in maximum, minimum, and mean LST. During the day we only observed increasing LST in the minimum parcel temperatures and, therefore, no correction was needed. At night, we observed a significant cooling in the maximum, minimum, and mean parcel temperatures over the flight periods. We used linear regression to identify the rate of cooling and then corrected all parcel temperatures to the median sampling time (approximately 1 am local time). Subsequent analyses conducted using both time-corrected and uncorrected data had consistent results for correlation analyses and significance tests.

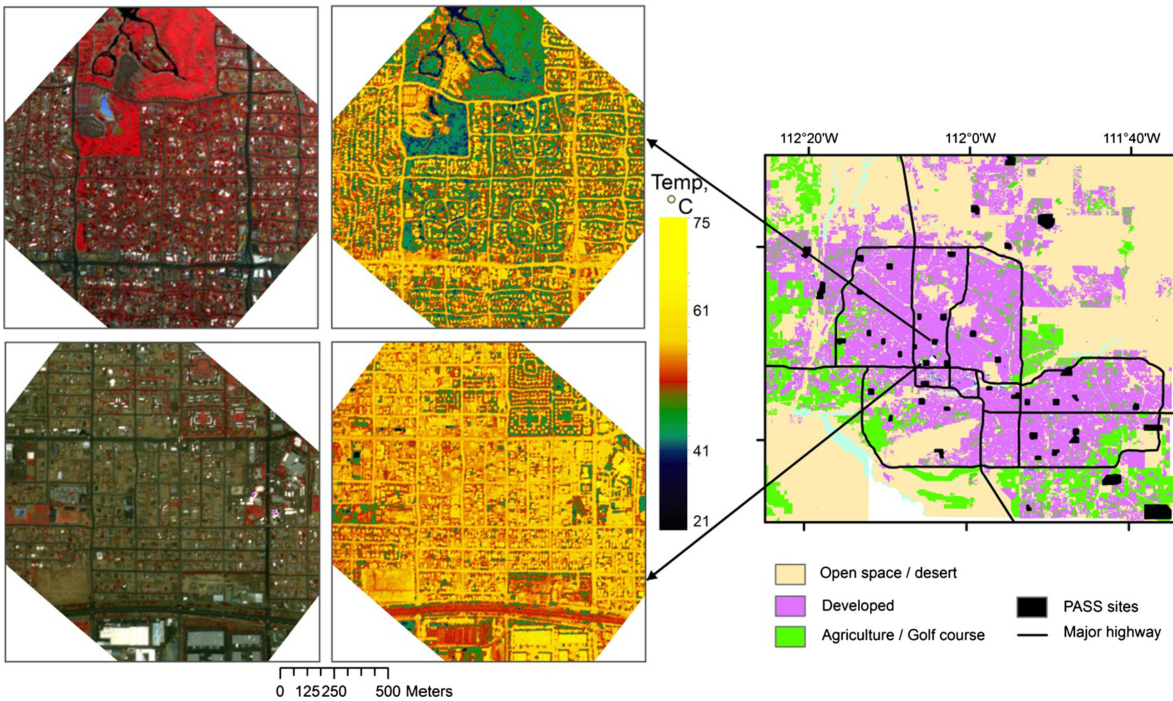

Fig. 1 Representative MASTER LST measurements for a highly vegetated neighborhood (*upper*) and minimally vegetated neighborhood (*lower*). MASTER bands 9, 5, and 3 were used for RGB display shown as false-color composites on the *left*

Analysis

We used a suite of standard statistical tools including correlations, linear regressions, and generalized liner models (GLM) for data analysis; all statistical analyses were conducted in Matlab 2013 (The Mathworks, Natick, MA). For each individual residential parcel we determined the means of LST, NDVI, and albedo and proportions of each land cover type. We analyzed the relationships between LST and the proportions of tree, grass, built, and road area at the parcel scale using a non-spatial linear correlation analysis. Because there are many thousands of parcels, all results at the parcel scale were statistically significant, consistent with most "big-data" analyses and, therefore, we focused on effect sizes in these analyses (Nuzzo 2014).

We also conducted analyses that compared parcel variation in LST between different neighborhoods. We computed regressions between mean parcel LST and NDVI within each single neighborhood in order to compare differences in vegetated cooling between neighborhoods. We compared expected bare surface temperatures (i.e. the intercepts of the linear regressions) with the LST-cooling effectiveness of vegetation (i.e. the slopes of the NDVI-LST regressions). This analysis showed the relative sensitivity of LST to vegetation abundance across neighborhoods.

We examined survey responses at the parcel scale and compared mean parcel LST for the group of respondents who reported symptoms of heat illness with the group reporting no symptoms. To account for differences in capacity to cope with heat, we restricted some analyses to the subsample of respondents who reported an impediment to using home air conditioning. These analyses were conducted using GLM for binomial distributions. At the neighborhood scale we used regression to evaluate the effects of mean neighborhood LST and land cover characteristics on aggregate measures (means) of respondents' perceptions of the local landscape and experiences of heat illness symptoms.

Results

Parcel land cover and LST relationships

Mean LST of individual residential parcels varied tremendously: daytime parcels ranged between 35.1

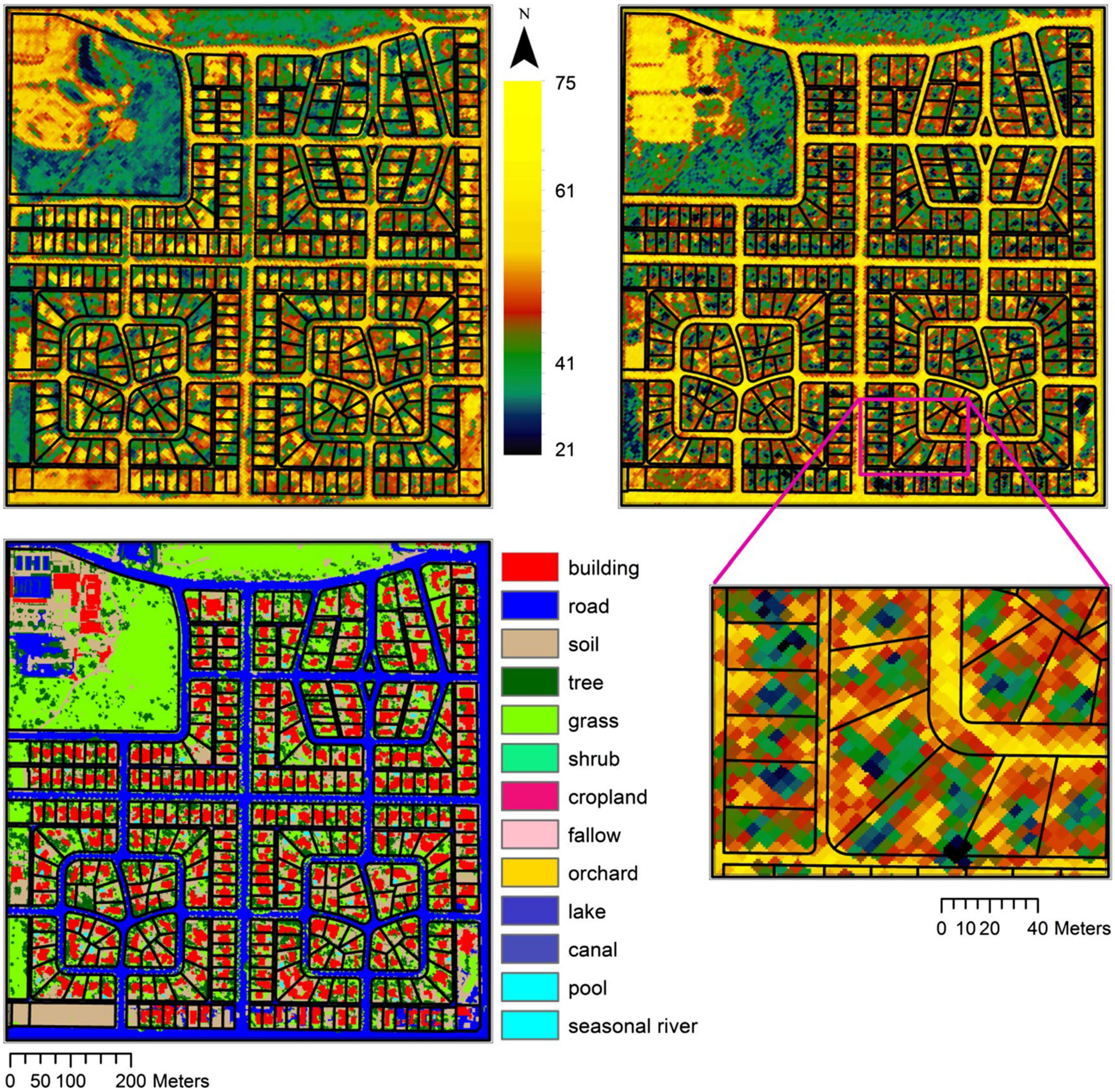

Fig. 2 Representative overlay of land cover data, parcel boundaries, and MASTER LST measurements for a highly vegetated neighborhood. The *upper left* and *upper right* show day and night time LST (°C) and parcel boundaries. The *lower left* shows land-cover classification and parcel boundaries. The *lower right* shows a detail subset of the nighttime LST and parcel delineations

and 67.4 °C and nighttime parcels ranged between 15.1 and 32.1 °C.

At the parcel scale, some measures of residential land cover were correlated with LST. During the daytime (Fig. 3), parcel-scale mean LST was inversely correlated with vegetation density. This finding was supported across three different measures of vegetation density: mean NDVI and the proportions of tree or grass cover. Tree cover had the highest correlation with LST ($r = -0.44$) and grass cover had the lowest correlation ($r = -0.27$). Built surface area, including roads, and albedo were weakly positively associated with mean daytime parcel LST. At night (Fig. 4) many of the relationships were reversed. Vegetation, quantified as NDVI, tree area, or grass area, was weakly positively associated with nighttime LST. As in the daytime, tree area had the highest of these correlations at night, although the relationship

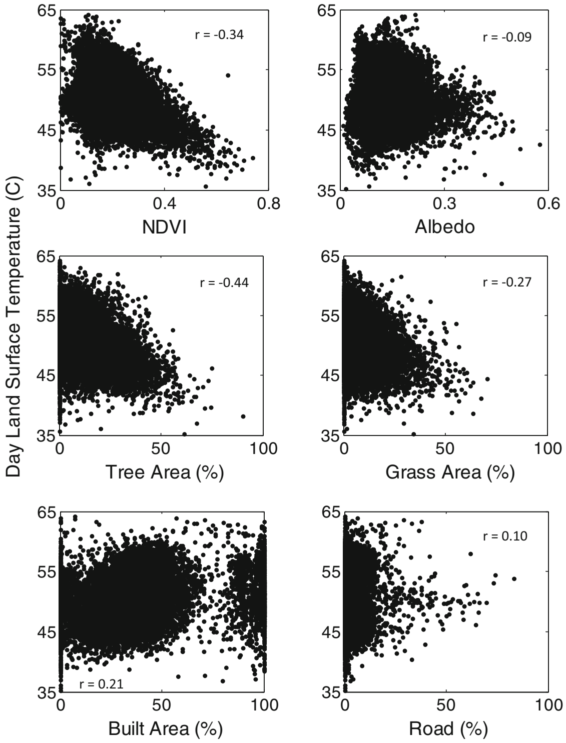

Fig. 3 Parcel scale relationships between land cover characteristics and daytime land surface temperature. Pearson correlation coefficients are shown for all relationships

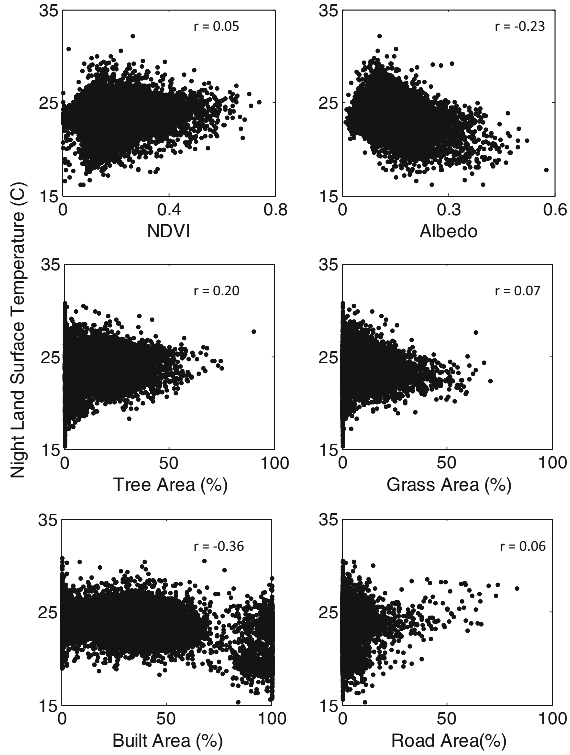

Fig. 4 Parcel scale relationships between land cover characteristics and nighttime land surface temperature. Pearson correlation coefficients are shown for all relationships

with LST was much weaker at night than in the day ($r = 0.20$). Larger areas of built surfaces and higher albedo were associated with cooler residential parcel LST at night ($r = -0.36$ and -0.23, respectively). Roads were minimally positively associated with nighttime LST. For all of these daytime and nighttime relationships there were large amounts of unexplained variation in mean LST at the parcel scale.

Regressions of parcel daytime LST on NDVI calculated independently for each neighborhood revealed that vegetation had a significant cooling effect within all neighborhoods. The magnitude of these effects, however, varied tremendously between neighborhoods. The slope magnitude between LST and NDVI in Fig. 5 is a quantification of the cooling effectiveness for differences in NDVI between the neighborhoods. Notably, the slope was strongly related to the regression intercept for each neighborhood, such that vegetation was more effective at cooling hotter neighborhoods ($p < 0.001$; $R^2 = 0.54$).

Neighborhood land cover, LST and household income

Consistent with previous findings in the Phoenix region, more impoverished neighborhoods were hotter ($r = 0.47$, $p < 0.01$; proportion of neighborhood households living below the federal poverty line and mean residential parcel daytime LST) and had less vegetation ($r = -0.45$; proportion of households in poverty and proportional cover of both grass and trees in parcels). Mean neighborhood daytime LST was inversely correlated with vegetation ($r = -0.37$, $p < 0.01$; proportion of neighborhood tree and grass area with mean daytime LST).

Micro-scale environments, residents' perceptions, and symptoms of heat illness

Mean daytime LST in the PASS neighborhoods ranged from 40 to 55 °C, tree area varied from 1.2 to 26.8 %, and road area varied from 3.7 to 53 %. Survey

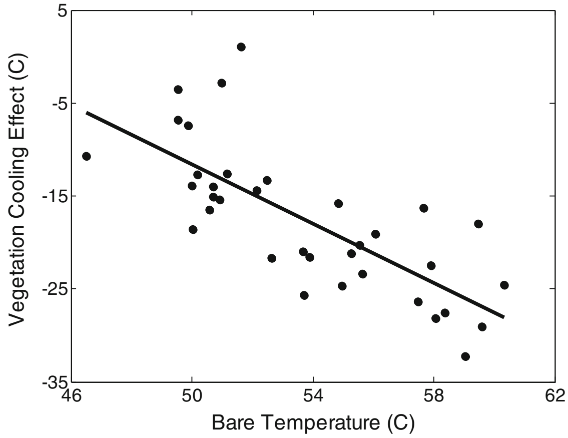

Fig. 5 Neighborhood variation in average parcel-scale daytime vegetative cooling (quantified as the regression slope between NDVI and LST) effect in relation to projected bare surface temperature (regression $p < 0.001$, $R^2 = 0.54$). Each datum represents a single neighborhood

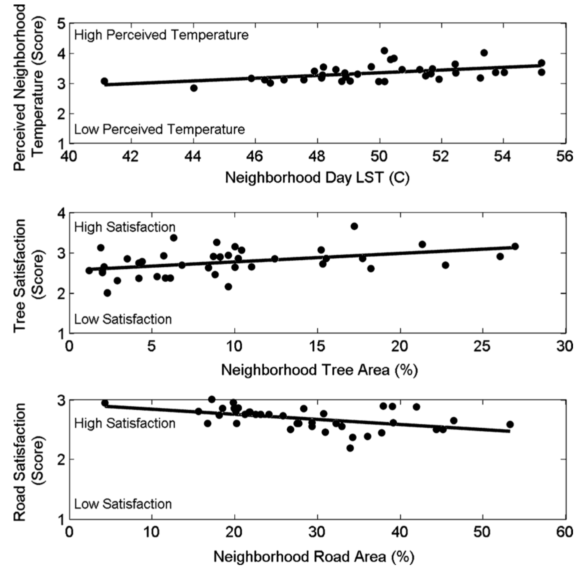

Fig. 6 PASS respondents' perceptions of their neighborhoods and neighborhood conditions observed by MASTER. *Upper panel* shows mean perception of relative neighborhood temperature and observed daytime neighborhood mean temperature ($p = 0.002$; $R^2 = 0.23$). *Middle panel* shows mean satisfaction with neighborhood trees and neighborhood tree area ($p < 0.006$; $R^2 = 0.18$). *Lower panel* shows mean satisfaction with amount of roads and paved area ($p = 0.002$; $R^2 = 0.23$). For *all panels* the scale of y-axis represents range of possible survey answers. Each datum represents a single neighborhood

respondents also varied widely in their perceptions of neighborhood environmental conditions and they used the full spectrum of available answers for the survey questions (Table 2). Residents' perceptions of temperature and land cover correlated with empirical observations of these characteristics (Fig. 6). Residents' mean perception of neighborhood temperature relative to other neighborhoods on a five-point scale (higher values indicate a hotter neighborhood) was higher in neighborhoods with higher daytime LST ($p = 0.002$, $R^2 = 0.23$). No relationship was detected between perception of relative neighborhood temperature and nighttime LST ($p > 0.3$). Perceptions of drivers of LST were also consistent with observed data. Residents' mean satisfaction with shade trees in their neighborhood on a four-point scale (higher values indicate more satisfaction) was positively related to percentage of neighborhood area covered by trees ($p = 0.006$, $R^2 = 0.18$). Residents' mean perception of the magnitude of paved surfaces as a neighborhood problem on a three-point scale (higher values indicate smaller problem, thus higher satisfaction) was negatively related to road area ($p = 0.002$, $R^2 = 0.23$).

The frequency of self-reported heat- related symptoms was correlated with daytime LST at both the parcel and neighborhood scales. The mean parcel daytime LST was significantly higher (0.93 °C, $p < 0.001$) for respondents who reported a heat-related illness in their household than for those reporting no heat related illnesses (Table 3). Furthermore, within the subgroup of respondents who had impediments to using home air conditioning, the parcel daytime LST difference between those who reported heat illness and those who did not was more than 50 % higher (1.52 °C, $p < 0.001$) than in the whole sample. This means the effect of parcel daytime surface temperature on heat illness was greater for people with reduced access to home air conditioning. The relationship between parcel nighttime LST and reported heat illness was not statistically significant for the whole sample or for the subgroup with restricted access to air conditioning. Daytime maximum air temperature on the day of survey completion did not have a statistically significant effect on the likelihood of reporting heat symptoms, indicating that it did not affect the results of our study.

At the neighborhood scale, the incidence of experiencing heat illness varied between 5 and 53 % of residents. An exponential increase in the rate of

Table 3 Differences in parcel land surface and air temperature (°C) between groups of PASS respondents who reported yes or no for experiencing household heat-related illnesses in the summer of 2010

	Temperature metric (°C)	No heat illness symptoms	Heat illness symptoms	GLM p value
All respondents	Daytime LST mean	49.05 (3.71)	49.98 (3.83)	$p < 0.001$
	Nighttime LST mean	23.95 (1.66)	23.84 (1.71)	$p = 0.107$
	Maximum T_{air} day of survey	35.98 (9.23)	35.12 (9.85)	$p = 0.258$
Reduced access to air conditioning	Daytime LST mean	48.60 (3.67)	50.12 (4.15)	$p < 0.001$
	Nighttime LST mean	23.92 (1.77)	23.92 (1.67)	$p = 0.197$
	Maximum T_{air} day of survey	35.75 (8.91)	37.28 (8.25)	$p = 0.491$

Values in cells represent means (standard deviations) of temperature for the individual parcels of respondents during daytime, means (standard deviations) of temperature for the individual parcels of respondents during the nighttime, and the maximum air temperature at Sky Harbor Airport on the day of survey response. The upper panel represents the 2011 PASS sample. The lower panel represents PASS respondents who reported an impediment to using air conditioning in their home (too expensive to operate, broken unit, etc.). Statistical significance was assessed through a GLM for binomial distribution

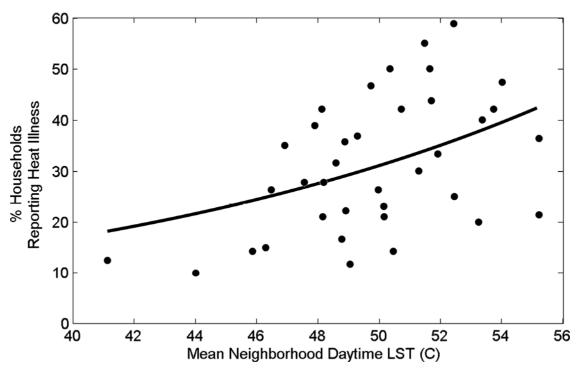

Fig. 7 Proportion of PASS respondents reporting someone in their household had suffered from symptoms related to heat illness during summer and corresponding neighborhood mean daytime LST (exponential regression; $p = 0.011$; $R^2 = 0.42$). Each datum represents a single neighborhood

reported heat-related illness was associated with neighborhood daytime LST (Fig. 7, $p = 0.011$; $R^2 = 0.42$). Variation in nighttime LST was not correlated with reported symptoms of heat-related illness at the neighborhood scale ($p > 0.1$).

Discussion

Fine resolution LST data coupled with comprehensive land cover maps, household surveys, and residential parcel delineations provide a robust description of the biophysical environment of homes and experiences with heat of the occupants. In this first parcel scale evaluation of land cover composition and LST variation, our results showed large differences in day and night LST accompanied by moderate couplings of LST with some land cover characteristics that differed between day and night. There was consistency between residents' perceptions of their neighborhood environments and empirically measured temperature and land covers. Using self-reported symptoms of heat illnesses, we found heat-related health impacts in the Phoenix region were positively associated with daytime LST of the respondent's residential parcel and with neighborhood daytime LST.

Improving understanding of parcel and neighborhood LST variation

Both daytime and nighttime surface temperatures were influenced by characteristics of the vegetated and built land covers at the parcel scale, which is consistent with previous findings at neighborhood scales (Weng et al. 2011; Myint et al. 2013). Of importance for designing heat mitigation strategies, the magnitude and direction of the relationships differed between day and night. Strategies to reduce day and night LST may differ in their effectiveness or even be in opposition. The hypothesis that vegetation-based LST cooling during the day is dominated by evaporative energy partitioning was supported by consistent results for all the greenness metrics—NDVI mean and percentages of tree cover or grass cover. Among these different vegetation variables, tree cover was the strongest correlate, which supports previous findings that grass is less effective than tree canopy for LST cooling (Myint et al. 2013), likely because trees with deeper roots have more consistent access to water and thereby maintain more cooling capacity. Our finding of a small positive nighttime parcel vegetation-LST relationship contrasts with previous results from Phoenix conducted at much larger (90 m pixels) scales (Buyantuyev and Wu 2010; Myint et al. 2013), which showed negative relationships between vegetation and LST during both the day and night. Also in contrast to regional UHI studies in this hot semi-arid environment (Myint et al. 2015), parcel scale built land covers were negatively related to nighttime LST. These reversals of daytime patterns at night suggests that at the very local scale, vegetation traps heat and building roofs more rapidly lose heat at night. Resolving these scale differences are an important research need. The negative relationship between albedo and nighttime LST and a smaller cooling effect of albedo throughout the day is consistent with an explanation that higher albedo surfaces have reduced energy storage and are therefore cooler early in the night. For parcel-scale land surface cooling, our results support both the use of vegetation and high albedo (e.g. white roofing) building materials (Georgescu et al. 2014). Because of generally stronger land cover—LST relationships during the day, peak temperatures may be more easily managed than nighttime minimum temperatures through landscape modification.

Notably, the effectiveness of vegetation (measured either as NDVI or vegetated area) on moderating temperatures varied substantially across neighborhoods. Although prior work has shown a cooling capacity for vegetation, it is generally believed that this capacity is regulated primarily by the area of vegetation (e.g. Jenerette et al. 2011; Li et al. 2011). Our findings suggest that, in addition to the area of vegetation, other factors influence the cooling capacity of vegetation, which we quantified as slope of LST-NDVI relationship within a neighborhood. We showed that vegetation cooling effectiveness at the parcel scale was correlated with expected bare surface temperature, which is consistent with prior neighborhood analyses examining patterns across seasons (Jenerette et al. 2011; Zhou et al. 2014). These findings suggest increased transpiration rates associated with hotter environments may lead to enhanced cooling. However, the effectiveness of vegetation may also be regulated by other factors we did not examine, including irrigation (Jenerette et al. 2011), landscape configuration (Connors et al. 2013; Zheng et al. 2014; Zhou et al. 2014), and plant species characteristics (Lundholm et al. 2010; McCarthy et al. 2011). Strategies for reducing LST through increased planting should be targeted toward areas with the highest temperatures because in these locations mitigation is likely to be more effective than planting in areas with lower LST.

Connecting environment with heat vulnerability

Daytime LST at neighborhood and parcel scales were correlated with residents' perceptions of the heat-related risk factors and heat-related symptoms of illness. Residents recognized regional variation in temperature and were similarly aware of important drivers of local LST including tree and road cover area in their surroundings. Such consistencies between perceptions and environment were previously suggested by comparisons with modeled air temperature data (Ruddell et al. 2012), although we present the first data-based comparison of perception-environment linkages for LST urban microclimates. The consistency between perceptions of factors associated with heat-related health risks and observed patterns of these drivers suggest there is value in consulting residents about their views of effective heat mitigation strategies.

Critical for understanding residents' heat vulnerability, we showed that both parcel and neighborhood daytime LSTs were correlated with self-reported symptoms of heat-related illnesses. Symptoms are markers of specific heat-health effects that provide more information about the broader health impacts of heat than can be gleaned from retrospective analysis of mortality and morbidity records. The incidence of self-reported heat illness symptoms in our sample greatly exceeded the frequencies of deaths and hospitalizations attributed to heat in the Phoenix region (Petitti et al. 2015).

Heat-related illnesses are associated with a suite of individual, social, and environmental factors that are themselves strongly interrelated (Reid et al. 2009; Hondula et al. 2012; Harlan et al. 2013; Petitti et al. 2015). The causal mechanisms leading to heat illnesses and deaths are not fully understood, although research is making progress in explaining linkages between spatial variations in living conditions and individual risks. For example, poverty is associated with chronic health problems that are exacerbated by heat (Balbus and Malina 2009), reduced coping capacities that include access to air conditioning (Reid et al. 2009), and elevated risks from working in higher temperature conditions (Petitti et al. 2013).

At present the correlations between LST and heat symptoms do not imply direct causation of heat illness but our study clearly shows that daytime LST can be one spatial indicator of heat risk. This was borne out in our analysis showing positive relationships between reported heat symptoms and daytime parcel and neighborhood LST, as well as a much stronger positive relationship between daytime parcel LST and symptoms of heat illness in the subsample of residents without consistent access to air conditioning (the most vulnerable subpopulation) compared to the entire population. Perhaps surprisingly, no similar correlations were observed between heat stress and nighttime LST in this setting.

Comparisons between LST and survey respondents' lived experiences were consistent with several of the few existing neighborhood scale studies, including Harlan et al. (2013) analysis of Phoenix, which showed an association between spatial variability in daytime LST and heat-related deaths. The present study also examined, but did not find, a relationship in this setting between mean parcel nighttime LST in mid-summer and the likelihood that survey respondents reported experiences with symptoms of heat illness. Our finding differs from a coarser-scale (1 km LST data) study in Paris, which found nighttime (minimum) LST was significantly associated with elderly heat deaths but there was no relationship between deaths and daytime (maximum) LST (Laaidi et al. 2012). More comparative research on spatial and temporal variability in surface temperatures and heat-related health outcomes in urban areas is needed.

Resolving the influence of daytime and nighttime temperature variations on health impacts at appropriate spatial and temporal scales is important for identifying effective landscape interventions that reduce health vulnerability. Yet a limitation of all temperature-related health studies, including our own, is the inability to make direct mechanistic links between the temperature metric, the time, and the site of where a heat-related health incident occurred. Some of the symptoms reported in our study undoubtedly occurred outside the home and neighborhood. Future work directed to individual microclimate monitoring (Kuras et al. 2015) will greatly improve the ability to make such temporal and spatial linkages.

Looking towards more heat resilient cities

Our findings highlight the potential value for microscale landscape interventions to reduce the heat exposure risk and vulnerability of urban residents. To meet current and future challenges of reducing urban heat vulnerability, cities are using four main strategies to manage heat risks: trees and vegetation, green roofs, cool roofs, and cool pavement (United States Environmental Protection Agency 2008). Georgescu et al. (2014) concluded from their model of the regional climate in Phoenix that more cool roofing materials would have a greater impact than more vegetation on decreasing regional air temperatures. However, for reducing health risks associated with higher LST, mitigating daytime LST in residential areas may be more effective than lowering nighttime air temperature in hot climates like Phoenix. At microscales, increasing greening in pedestrian pathways and outdoor play spaces may be especially useful (Vanos 2015). In comparing the relative cooling effectiveness of vegetation and albedo, our findings support increasing urban greening, especially by planting trees around homes with a large fraction of human-built land surfaces. Because the cooling effectiveness of increasing albedo was observed primarily at night, this strategy may not be as valuable for reducing heat-related illnesses. However, as trees in hot arid cities require irrigation, balancing the cooling benefits with water use is an essential sustainability challenge (Gober et al. 2010; Jenerette et al. 2011; Pataki et al. 2011). Increasing albedo does not have an associated water consumption trade-off and could more readily be implemented anywhere.

Reconciling the effectiveness of alternate mitigation strategies is an important challenge for reducing urban vulnerability to climate changes (Liang and Weng 2008; Georgescu et al. 2014). Current global demographic trends projecting 2.5 billion more urban residents by 2050, a 64 % increase from current distributions (United Nations Department of Economic and Social Affairs Population Division 2014), will place more people's health at risk from extreme heat due to combinations of global warming associated with greenhouse gas emissions and regional warming associated with UHIs (Intergovernmental Panel on Climate Change 2014). Interdisciplinary approaches such as this one, which geographically overlay data describing high resolution environmental and human variation at the scale of individual homes, provide a powerful lens for understanding and designing the coupled natural and human systems that contribute to reducing heat vulnerability.

Acknowledgments This work was supported by National Science Foundation Grants GEO-0816168, GEO-0814692, BCS-1026865, EF-1049251, EF-1049224, and DEB-0919006. We thank Anthony Brazel and Chris Martin for their advice on the MASTER data collection effort and David Hondoula for insightful discussions. All data are available from CAP-LTER (caplter.asu.edu).

References

American Association for Public Opinion Research (2008) Standard definitions: final dispositions of case codes and outcome rates for surveys (revised). http://www.aapor.org/AAPORKentico/Education-Resources/For-Researchers/Poll-Survey-FAQ/Response-Rates-An-Overview.aspx

Baatz M, Hoffmann C, Willhauck G (2008) Progressing from object-based to object-oriented image analysis. In: Blaschke T, Lang S, Hay GJ (eds) Object-based image analysis: spatial concepts for knowledge-driven remote sensing applications. Springer, Berlin, pp 29–42

Balbus JM, Malina C (2009) Identifying vulnerable subpopulations for climate change health effects in the United States. J Occup Environ Med 51:33–37

Basu R, Samet JM (2002) Relation between elevated ambient temperature and mortality: a review of the epidemiologic evidence. Epidemiol Rev 24:190–202

Belanger D, Gosselin P, Valois P, Abdous B (2015) Neighbourhood and dwelling characteristics associated with the self-reported adverse health effects of heat in most deprived urban areas: a cross-sectional study in 9 cities. Health Place 32:8–18

Bernstein LS, Adler-Golden SM, Sundberg RL, Levine RY, Perkins TC, Berk A, Ratkowski AJ, Felde G, Hoke ML (2005) Validation of the quick atmospheric correction (QUAC) algorithm for VNIR-SWIR multi- and hyperspectral imagery. In: SPIE proceedings, algorithms and technologies for multispectral, hyperspectral, and ultraspectral imagery XI, pp 668–678

Buscail C, Upegui E, Viel JF (2012) Mapping heatwave health risk at the community level for public health action. Int J Health Geogr. doi:10.1186/1476-1072x-1111-1138

Buyantuyev A, Wu JG (2010) Urban heat islands and landscape heterogeneity: linking spatiotemporal variations in surface temperatures to land-cover and socioeconomic patterns. Landscape Ecol 25:17–33

Cao X, Onishi A, Chen J, Imura H (2010) Quantifying the cool island intensity of urban parks using ASTER and IKONOS data. Landsc Urban Plan 96:224–231

Chow WTL, Brennan D, Brazel AJ (2012) Urban heat island research in Phoenix, Arizona: theoretical Contributions and policy applications. Bull Am Meteorol Soc 93:517–530

Connors JP, Galletti CS, Chow WTL (2013) Landscape configuration and urban heat island effects: assessing the relationship between landscape characteristics and land surface temperature in Phoenix, Arizona. Landscape Ecol 28:271–283

Deng CB, Wu CS (2013) Examining the impacts of urban biophysical compositions on surface urban heat island: a spectral unmixing and thermal mixing approach. Remote Sens Environ 131:262–274

Elachi C (1987) Introduction to the physics and techniques of remote sensing. Wiley, New York

Georgescu M, Morefield PE, Bierwagen BG, Weaver CP (2014) Urban adaptation can roll back warming of emerging megapolitan regions. Proc Natl Acad Sci USA 111:2909–2914

Gober P, Brazel A, Quay R, Myint S, Grossman-Clarke S, Miller A, Rossi S (2010) Using watered landscapes to manipulate urban heat island effects: how much water will it take to cool Phoenix? J Am Plan Assoc 76:109–121

Goldreich Y (2006) Ground and top of canopy layer urban heat island partitioning on an airborne image. Remote Sens Environ 104:247–255

Grimm NB, Redman CL (2004) Approaches to the study of urban ecosystems: the case study of Central Arizona—Phoenix. Urban Ecosyst 7:199–213

Grove JM, Locke DH, O'Neil-Dunne JPM (2014) An ecology of prestige in New York City: examining the relationships among population density, socio-economic status, group identity, and residential canopy cover. Environ Manag 54:402–419

Harlan SL, Declet-Barreto JH, Stefanov WL, Petitti DB (2013) Neighborhood effects on heat deaths: social and environmental predictors of vulnerability in Maricopa County, Arizona. Environ Health Perspect 121:197–204

Hondula DM, Barnett AG (2014) Heat-related morbidity in Brisbane, Australia: spatial variation and area-level predictors. Environ Health Perspect 122:831–836

Hondula DM, Davis RE, Leisten MJ, Saha MV, Veazey LM, Wegner CR (2012) Fine-scale spatial variability of heat-related mortality in Philadelphia County, USA, from 1983-2008: a case-series analysis. Environ Health. doi:10.1186/1476-1069x-1111-1116

Hook SJ, Myers JEJ, Thome KJ, Fitzgerald M, Kahle AB (2001) The MODIS/ASTER airborne simulator (MASTER)—a new instrument for earth science studies. Remote Sens Environ 76:93–102

Imhoff ML, Zhang P, Wolfe RE, Bounoua L (2010) Remote sensing of the urban heat island effect across biomes in the continental USA. Remote Sens Environ 114:504–513

Intergovernmental Panel on Climate Change (2014) Climate change 2014: impacts, adaptation, and vulnerability. Cambridge University Press, Cambridge

Jenerette GD, Harlan SL, Brazel A, Jones N, Larsen L, Stefanov WL (2007) Regional relationships between surface temperature, vegetation, and human settlement in a rapidly urbanizing ecosystem. Landscape Ecol 22:353–365

Jenerette GD, Harlan SL, Stefanov WL, Martin CA (2011) Ecosystem services and urban heat riskscape moderation: water, green spaces, and social inequality in Phoenix, USA. Ecol Appl 21:2637–2651

Jenerette GD, Miller G, Buyantuev A, Pataki DE, Gillespie T, Pincetl S (2013) Urban vegetation and income segregation in drylands: a synthesis of seven metropolitan regions in the southwestern United States. Environ Res Lett 8:044001

Johnson BR, Young SJ (1998) In-scene atmospheric compensation: application to SEBASS data collected at the ARM site. The Aerospace Corporation

Johnson DP, Wilson JS, Luber GC (2009) Socioeconomic indicators of heat-related health risk supplemented with remotely sensed data. Int J Health Geogr. doi:10.1186/1476-1072x-1188-1157

Johnson DP, Stanforth A, Lulla V, Luber G (2012) Developing an applied extreme heat vulnerability index utilizing socioeconomic and environmental data. Appl Geogr 35:23–31

Kalkstein LS (1991) A new approach to evaluate the impact of climate on human mortality. Environ Health Perspect 96:145–150

Kalma JD, McVicar TR, McCabe MF (2008) Estimating land surface evaporation: a review of methods using remotely sensed surface temperature data. Surv Geophys 29:421–469

Kealy PS, Hook SJ (1993) Separating temperature and emissivity in thermal infrared multispectral scanner data—Implications for recovering land-surface temperatures. IEEE Trans Geosci Remote Sens 31:1155–1164

Kuras ER, Hondula DM, Brown-Saracino J (2015) Heterogeneity in individually experienced temperatures (IETs) within an urban neighborhood: insights from a new approach to measuring heat exposure. Int J Biometeorol. doi:10.1007/s00484-00014-00946-x

Kustas W, Anderson M (2009) Advances in thermal infrared remote sensing for land surface modeling. Agric For Meteorol 149:2071–2081

Laaidi K, Zeghnoun A, Dousset B, Bretin P, Vandentorren S, Giraudet E, Beaudeau P (2012) The impact of heat islands on mortality in Paris during the August 2003 heat wave. Environ Health Perspect 120:254–259

Lee S (2015) Self-rated health in health surveys. In: Johnson TP (ed) Handbook of health survey methods. Wiley, Hoboken

Li JX, Song CH, Cao L, Zhu FG, Meng XL, Wu JG (2011) Impacts of landscape structure on surface urban heat islands: a case study of Shanghai, China. Remote Sens Environ 115:3249–3263

Li X, Myint SW, Zhang Y, Galletti C, Zhang X, Turner Ii BL (2014) Object-based land-cover classification for metropolitan Phoenix, Arizona, using aerial photography. Int J Appl Earth Obs Geoinf 33:321–330

Liang SL (2001) Narrowband to broadband conversions of land surface albedo I: algorithms. Remote Sens Environ 76: 213–238

Liang BQ, Weng QH (2008) Multiscale analysis of census-based land surface temperature variations and determinants in Indianapolis, United States. J Urban Plan Dev 134: 129–139

Lundholm J, MacIvor JS, MacDougall Z, Ranalli M (2010) Plant species and functional group combinations affect green roof ecosystem functions. PLoS One. doi:10.1371/journal.pone.0009677

McCarthy HR, Pataki DE, Jenerette GD (2011) Plant water-use efficiency as a metric of urban ecosystem services. Ecol Appl 21:3115–3127

Myint SW, Gober P, Brazel A, Grossman-Clarke S, Weng QH (2011) Per-pixel vs. object-based classification of urban land cover extraction using high spatial resolution imagery. Remote Sens Environ 115:1145–1161

Myint SW, Wentz EA, Brazel AJ, Quattrochi DA (2013) The impact of distinct anthropogenic and vegetation features on urban warming. Landscape Ecol 28:959–978

Myint SW, Zheng B, Talen E, Fan C, Kaplan S, Middel A, Smith M, Huang HP, Brazel A (2015) Does the spatial arrangement of urban landscape matter? Examples of urban warming and cooling in Phoenix and Las Vegas. Ecosystem Health and Sustainability 1:art15

Nuzzo R (2014) Statistical errors. Nature 506:150–152

Oke TR (1973) City size and urban heat island. Atmos Environ 7:769–779

Pataki DE, Boone CG, Hogue TS, Jenerette GD, McFadden JP, Pincetl S (2011) Ecohydrology bearings-invited commentary socio-ecohydrology and the urban water challenge. Ecohydrology 4:341–347

Peng SS, Piao SL, Ciais P, Friedlingstein P, Ottle C, Breon FM, Nan HJ, Zhou LM, Myneni RB (2012) Surface urban heat island across 419 global big cities. Environ Sci Technol 46:696–703

Petitti DB, Harlan SL, Chowell-Puente G, Ruddell D (2013) Occupation and environmental heat-associated deaths in Maricopa County, Arizona: a case-control study. PLoS One 8:e62596

Petitti DB, Hondula DM, Yang S, Harlan SL, Chowell G (2015) Multiple trigger points for quantifying heat-health impacts: new evidence from a hot climate. Environ Health Perspect. doi:10.1289/ehp.1409119

Reid CE, O'Neill MS, Gronlund CJ, Brines SJ, Brown DG, Diez-Roux AV, Schwartz J (2009) Mapping community determinants of heat vulnerability. Environ Health Perspect 117:1730–1736

Ruddell D, Harlan SL, Grossman-Clarke S, Chowell G (2012) Scales of perception: public awareness of regional and neighborhood climates. Clim Change 111:581–607

Small C (2003) High spatial resolution spectral mixture analysis of urban reflectance. Remote Sens Environ 88:170–186

Song J, Du S, Feng X, Guo L (2014) The relationships between landscape compositions and land surface temperature: quantifying their resolution sensitivity with spatial regression models. Landsc Urban Plan 123:145–157

Stone B Jr (2012) The city and the coming climate: climate change in the places we live. Cambridge University Press, New York

Tucker CJ (1979) Red and photographic infrared linear combinations for monitoring vegetation. Remote Sens Environ 8:127–150

Uejio CK, Wilhelmi OV, Golden JS, Mills DM, Gulino SP, Samenow JP (2011) Intra-urban societal vulnerability to extreme heat: the role of heat exposure and the built environment, socioeconomics, and neighborhood stability. Health Place 17:498–507

United States Environmental Protection Agency (2006) Excessive heat events guidebook. EPA 430-B-06-005 (June). http://www.epa.gov/heatisland/about/pdf/EHEguide_final.pdf

United States Environmental Protection Agency (2008) Chapter 1 Heat island basics in reducing urban heat islands: compendium of strategies. http://www.epa.gov/heatisland/resources/compendium.htm

United Nations Department of Economic and Social Affairs Population Division (2014) World urbanization prospects: the 2014 revision, highlights (ST/ESA/SER.A/352)

Vanos JK (2015) Children's health and vulnerability in outdoor microclimates: a comprehensive review. Environ Int 76:1–15

Voogt JA, Oke TR (2003) Thermal remote sensing of urban climates. Remote Sens Environ 86:370–384

Weng QH, Rajasekar U, Hu XF (2011) Modeling urban heat islands and their relationship with impervious surface and vegetation abundance by using ASTER images. IEEE Trans Geosci Remote Sens 49:4080–4089

Xiang TT, Vivoni ER, Gochis DJ (2014) Seasonal evolution of ecohydrological controls on land surface temperature over complex terrain. Water Resour Res 50:3852–3874

Zhan WF, Chen YH, Zhou J, Wang JF, Liu WY, Voogt J, Zhu XL, Quan JL, Li J (2013) Disaggregation of remotely sensed land surface temperature: literature survey, taxonomy, issues, and caveats. Remote Sens Environ 131:119–139

Zheng B, Myint SW, Fan C (2014) Spatial configuration of anthropogenic land cover impacts on urban warming. Landsc Urban Plan 103:104–111

Zhou WQ, Huang GL, Cadenasso ML (2011) Does spatial configuration matter? Understanding the effects of land cover pattern on land surface temperature in urban landscapes. Landsc Urban Plan 102:54–63

Zhou WQ, Qian YG, Li XM, Li WF, Han LJ (2014) Relationships between land cover and the surface urban heat island: seasonal variability and effects of spatial and thematic resolution of land cover data on predicting land surface temperatures. Landscape Ecol 29:153–167